

# Evaluation of a single transect method for collecting grape samples based on Sentinel-2 imagery for the characterization of overall vineyard performance

B.S. Sams<sup>1\*</sup>, M. Aboutalebi<sup>1</sup>, R.G.V. Bramley<sup>2</sup>, L.A. Sanchez<sup>1</sup>, and N.K. Dokoozlian<sup>1</sup>

<sup>1</sup>*Winegrowing Research, E&J Gallo Winery, Modesto, CA, USA*

<sup>2</sup>*CSIRO, Waite Campus, Locked Bag 2, Glen Osmond, SA 5064, Australia*

*\*Corresponding author (brent.sams@ejgallo.com)*

## Abstract

Commercial vineyards are streamed into different wine programs based on analysis of grape or juice samples collected from the field, but spatial and temporal variability can lead to sub-optimal tiering of grapes. This is a particularly difficult problem to overcome in the typically large vineyards of California's Central Valley. Due to economic and laboratory constraints on sample collection, processing, and analysis, a single sample is often expected to represent the overall fruit quality of a given vineyard. Recently, a sampling method was developed to account for the spatial variability of vineyards using remotely sensed imagery. This method, originally based on imagery from Landsat 7, attempts to find a set of three contiguous pixels in an image captured over a vineyard with normalized difference vegetation index (NDVI) values spanning different bins in a histogram analysis. The output was a single transect (3P) in each vineyard for sample collection. The objective of this study was to validate this method with imagery from the Sentinel-2 satellite constellation using maps of grape composition produced from a relatively high-density sampling project. In the 2017, 2018, and 2019 growing seasons, 125 samples were collected at harvest in each of four vineyards in the Lodi American Viticulture Area (AVA) to produce geostatistically rigorous maps of grape composition and served as the ground validation for the sampling method under investigation here. Results showed that in most cases, the total soluble solids (TSS) values extracted from the fruit composition maps in the single Sentinel-2 based transects were within an acceptable range (-1 to +1 °Brix) of the mean values of the 125 samples. The implementation of this method could save the winegrowing industry countless hours necessary for traditional sampling, processing, and analysis of fruit samples by incorporating spatial awareness into sampling plans.

**Keywords:** vineyard variability, sampling, precision agriculture, digital viticulture

## Introduction

Vineyard maturity sampling methods, the processes by which vineyard ripening is tracked to determine optimal harvest timing, varies considerably across organizations. Most rely on collecting grape clusters from as few as one and as many as 20 locations, and some try to sample based on some pre-existing knowledge of variability. However, sampling in this manner can be extremely costly and time consuming. Recently, a Landsat satellite imagery-based solution using a single sampling transect based on the distribution of pixel values was developed and evaluated for sugar sampling (Meyers et al. 2020). This method used histogram binning of the input raster values of the normalized difference vegetation index (NDVI) to find three contiguous 30 m Landsat pixels (90 m total transect) that would represent different sections of each histogram with the limitation of a single transect aligned with the orientation of vine rows in each vineyard. The quicker return interval and improved

spatial resolution from the European Space Agency's Sentinel program could allow for even smaller transects that could adequately represent the sugar variability in wine grape vineyards. The objective of this project was to validate this approach to vineyard sugar sampling using the higher resolution Sentinel 2 satellite imagery (10 m pixel resolution) for an even smaller transect (30 m total transect; 3P).

## Materials and Methods

### *Vineyards*

In the 2017, 2018, and 2019 growing seasons, 125 samples were collected within a few days prior to commercial harvest from each of four *Vitis vinifera* L. cv. Cabernet Sauvignon vineyards in the Lodi AVA in central California (38° 7' 44" N, 121° 16' 51" W). The vineyards and samples were the same as those in Sams et al. (2022a, b). All four vineyards were drip-irrigated, spur-pruned, and machine harvested. Vineyard A was planted on rootstock 039-16, clone FPS 08, in 2010 and has been pruned to a single bilateral sprawling training system with no inter-row cover crop. Vineyard B was planted on rootstock SO4, clone 7, in 2013. Vineyard C was planted on rootstock 1103P, clone 7, in 1998. Vineyards B and C were both trained to a quadrilateral sprawling system with a perennial inter-row grass cover crop. Vineyard D was planted on rootstock 039-16, clone 15, in 2012. Vineyard D was a mechanized high wire sprawling canopy and used the same inter-row cover crop as Vineyards B and C. Vineyards A and C varied by less than 2 m in elevation, while Vineyard B sloped approximately 20 m from north to south. Vineyard D had an elevation range of around 8 m and was characterized by rolling hills.

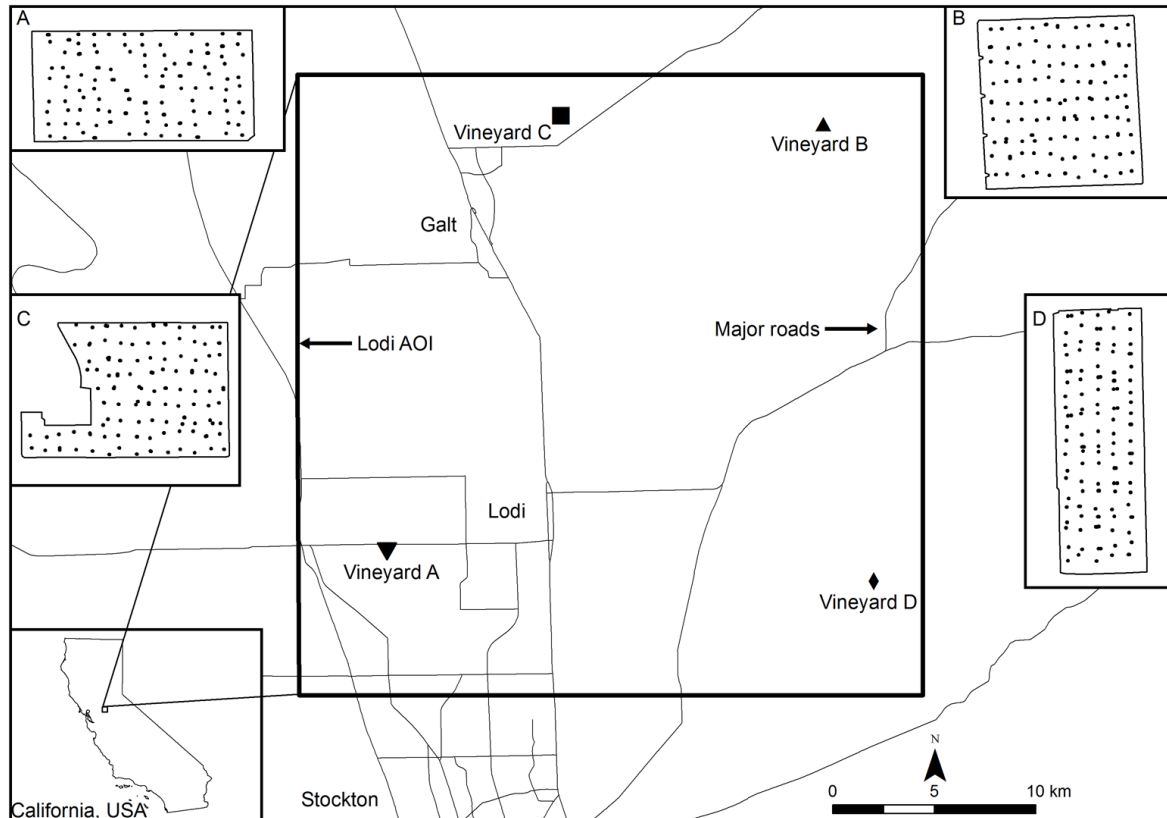


Figure 1. Vineyards and sample layouts used in the analysis (from Sams et al. 2022a).

Sams et al. (2022a) outlined the sampling design intended for spatial analysis of fruit chemistry and yield. This design used modified regular grids based on row and vine distance of each vineyard but with random offsets applied to each data vine location and allowed for the spatial dependence and variability to be characterized at uneven distances between samples for robust variogram generation.

Commercial harvest for the four vineyards occurred within 10 days of one another in all 3 years, with the entire 2019 sample collection occurring over just 5 calendar days. In most cases, the vineyards were sampled either the day before or on the day of commercial harvest. Fruit from each data vine was completely removed and yield for each vine recorded. Twenty bunches, sampled at random from each vine, were then set aside for laboratory analysis.

### *Laboratory*

Upon arrival at the laboratory, the collected samples of whole bunches were mechanically destemmed and homogenized prior to extraction with an acidified 50% ethanolic solution. A WineScan FT-120 Fourier Transform Infrared Spectroscopy (FOSS North America, Eden Prairie, MN, USA) was used to analyze total soluble solids (TSS). The calibration was created by WinISI II software (FOSS, Hillerød, Denmark) using E&J Gallo's internal grapes and reference chemistry quality standards.

### *Image analysis and data processing*

Sentinel 2 images from mid-June were downloaded and processed to compute the NDVI using Google Earth Engine (Gorelick et al. 2017). Digital boundaries of each vineyard were used to extract only those pixels which represented vineyard area and eliminated those from outside roads, buildings, trees, and other objects which could compromise the spectral signal of vines. An algorithm for determining the optimum single transect of three contiguous pixels (3P) representing as much variation in NDVI values as possible was calculated for each vineyard in each season. Figure 2 shows the workflow outlining the steps of the algorithm.

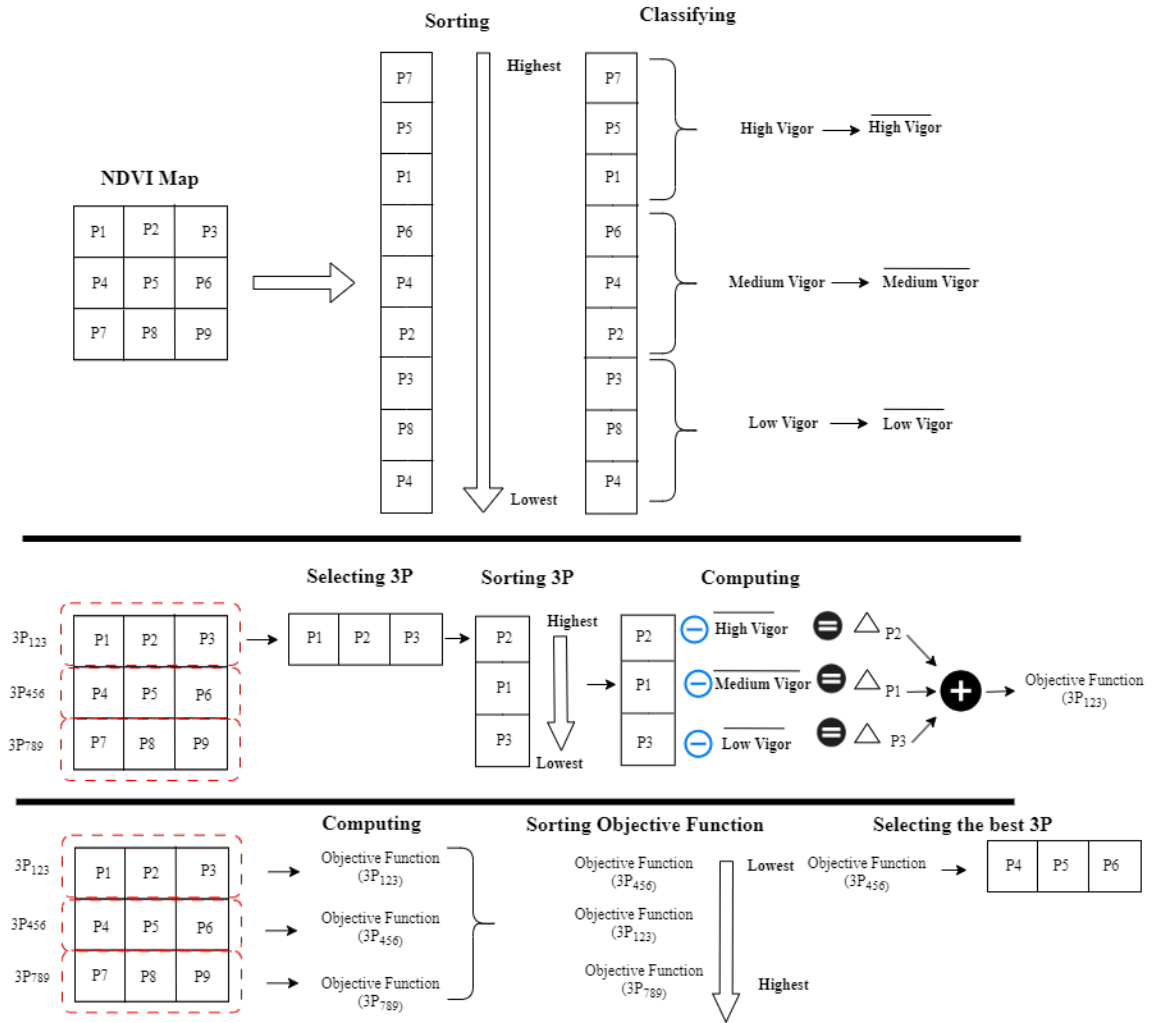


Figure 2. The workflow diagram of the three-pixel (3P) algorithm illustrating the procedure for selecting the best transect for sampling in vineyards using NDVI maps.

The algorithm begins by sorting the NDVI values from high to low. After sorting, it divides the NDVI values into the first, second, and third tertiles, which correspond to high, medium, and low vigor classes, respectively. Following this, the mean NDVI for each category is computed. The next step is to start scanning the NDVI map, selecting each 3P based on the row orientation (vertical for north to south, horizontal for east to west and diagonal for the rest). For each 3P, the algorithm sorts NDVI values from high to low and calculates the differences between the NDVI values of the 3P and the average vigor classes (high vigor, medium vigor, and low vigor). The sum of these differences is considered the score or objective function for this search problem. As shown in the workflow, this objective function can be mathematically defined as follows:

$$\text{Objective Function} : |P_{high} - \overline{High\ vigor}| + |P_{Med} - \overline{Medium\ vigor}| + |P_{low} - \overline{Low\ vigor}|$$

where  $P_{high}$ ,  $P_{med}$ ,  $P_{low}$  represent the high, medium, and low NDVI values of 3P, respectively. Based on this objective function, the optimal transect is identified by the smallest difference between the NDVI values of the 3P and the average vigor classes. Therefore, the 3P corresponding to the lowest value of the objective function indicates the optimal single transect.

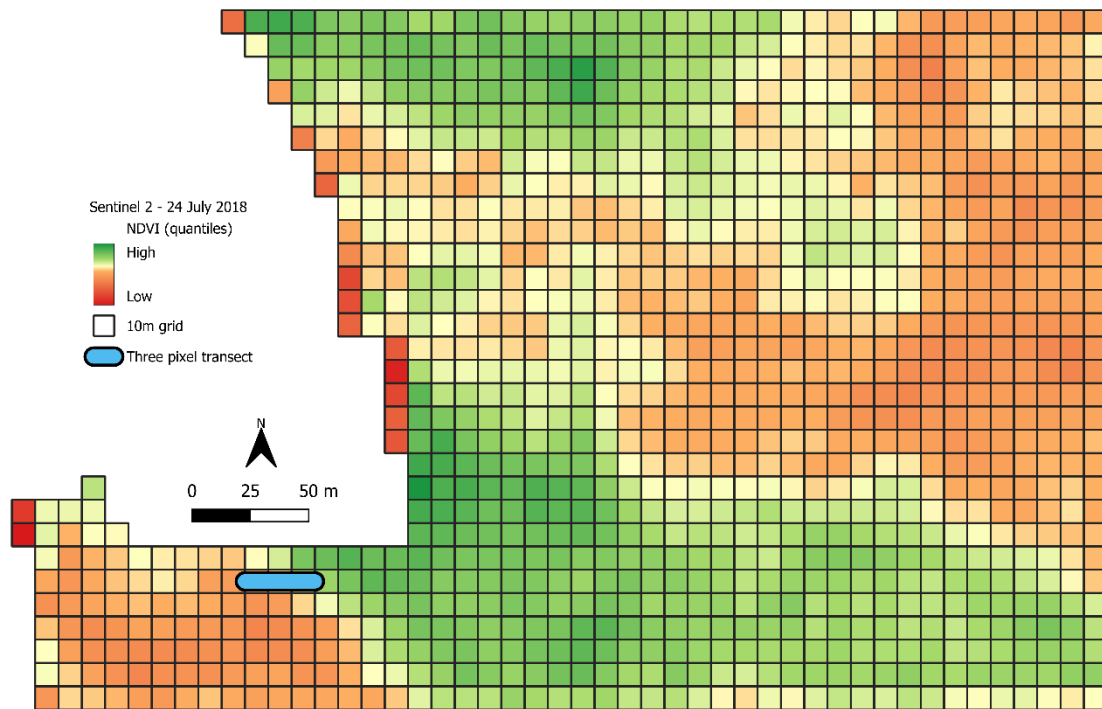


Figure 3. Gridded NDVI map from Sentinel 2 of Vineyard C showing the three-pixel (3P) line straddling different pixel values.

To produce maps of TSS, experimental variograms were estimated from the 125 samples per vineyard per season using a spherical model and maps were interpolated using global point kriging in VESPER (Minasny et al. 2005). Values of TSS from the 3P were extracted from the interpolated maps using the Sentinel 2 grids (Figure 4). The mean TSS value from the 3P transect was then compared against the histograms of TSS computed from the 125 samples collected from each vineyard in each season (Figure 5).

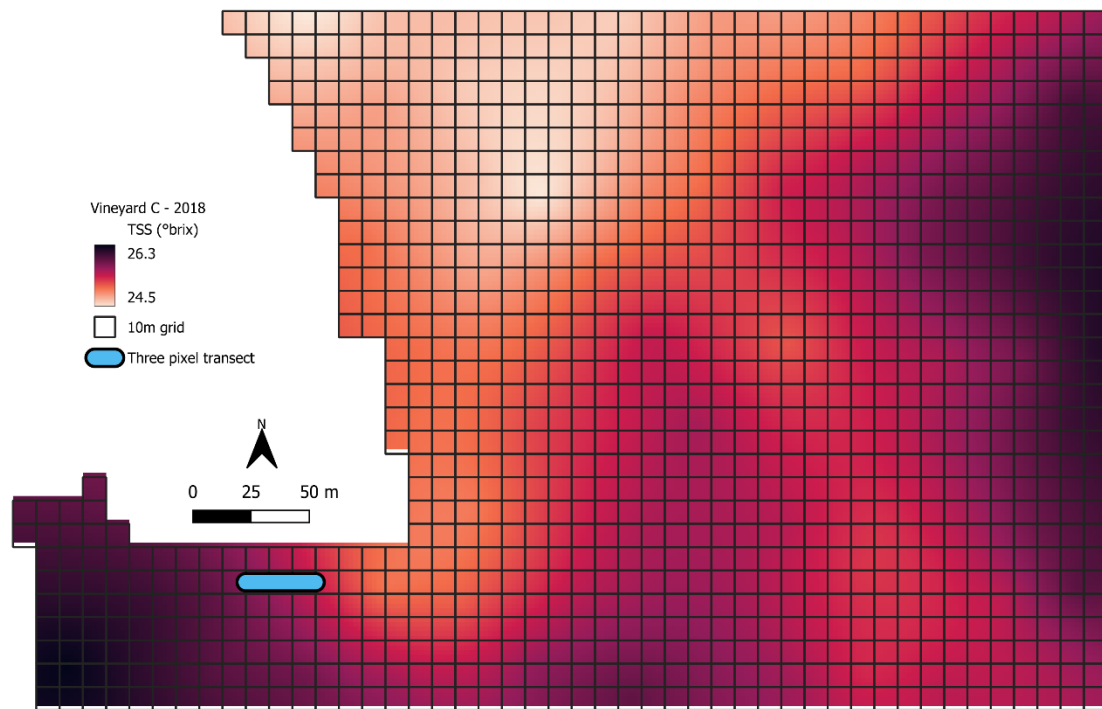


Figure 4. An example of the three-pixel transects overlaid on a map of total soluble solids (TSS).

## Results

Comparing the TSS histograms of the 125 sampling campaigns in 2017, 2018, and 2019 with the values extracted from the three pixel transects identified by the Sentinel 2 NDVI based sampling algorithm showed general consistency across vineyards and seasons (Figure 5). In most cases, the mean value from the three-pixel transects overlapped with the histogram peak of TSS. Exceptions include Vineyard B in 2017 and 2019 and Vineyard D in 2017, though all three of these were within one degree brix of the histogram peak. The TSS values in Table 1 confirm this consistency as none of the blocks in any season showed values outside of the standard deviation of the 125-sample average.

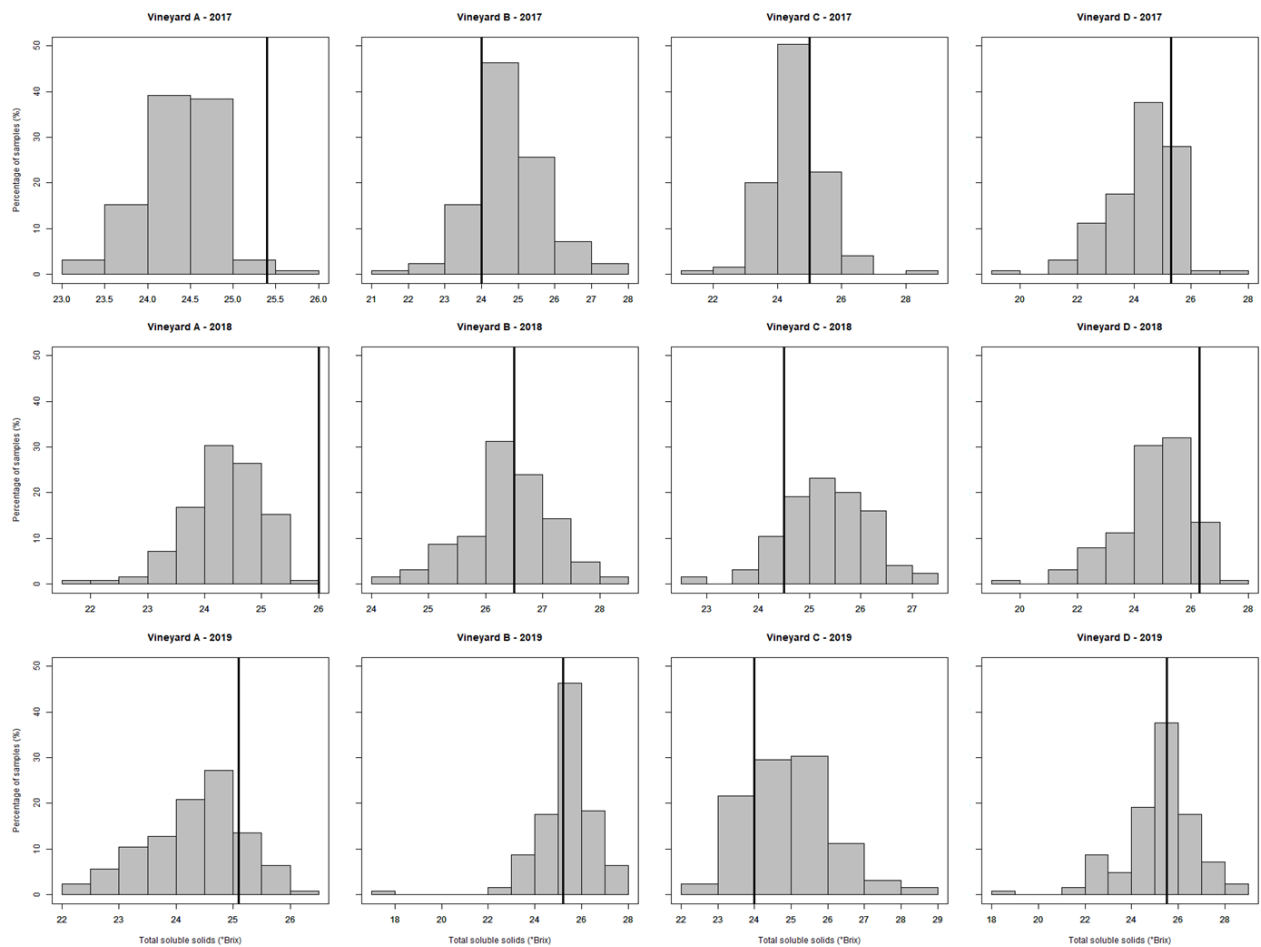


Figure 5. Histograms from the 125 sampling campaigns in 2017, 2018, and 2019 with the mean value extracted from maps of TSS in the three pixel transects based on Sentinel 2 NDVI. (Alternatively, this figure could be broken up into either 1) three figures, one per year with all four blocks OR 2) four figures, one per block with all three years.)

Table 1. Mean and standard deviation of total soluble solids from the 125 samples collected in each block and year and the values extracted from the interpolated maps using the three-pixel transect in each of the four vineyards from 2017-2019.

Vineyard	Total Soluble Solids (°Brix)					
	2017		2018		2019	
	Avg 125	3-pixel	Avg 125	3-pixel	Avg 125	3-pixel
A	24.4±0.5	24.4	24.4±0.7	24.3	24.4±0.8	24.6
B	24.8±1.0	23.8	26.5±0.8	26.3	25.4±1.3	24.8
C	24.6±0.9	24.1	25.4±0.8	25.5	25.0±1.2	25.5
D	24.3±1.2	23.8	24.7±1.4	25.0	25.3±1.6	25.8

## Discussion

Large growing operations or wineries with significant vineyard holdings/contracted vineyards must try to account for spatial variability with as little time and effort as possible, a process usually done through manual in-field sampling. Precision agriculture techniques show promise for variable rate management in wine grape vineyards, but smart implements designed to address variability have been slow to develop. Many tools are available for

characterizing spatial variability of yield and fruit quality, such as high-density field sampling (Bramley 2005; Sams et al. 2022a), yield monitors and mapping (Bramley 2001; Taylor et al. 2016), remotely sensed imagery from aircraft and satellites (Hall et al. 2011; Fiorillo et al. 2012; Sozzi et al. 2020), soil surveys (Bramley et al. 2011a; Sams et al. 2022b), and proximal sensing (Trought and Bramley 2011; Baluja et al. 2012; Gutiérrez et al. 2019), but very few solutions exist to react to this variability. Given this lack of options, viticulturists and receiving wineries must attempt to account for spatial variability of yield and fruit quality rather than try to eliminate it through variable rate practices since grapes from a given vineyard are typically streamed into a single wine program. Zonal sampling (Hall et al., 2002; Dorin et al., 2022), taking samples from zones of similar yield/quality, may be an option for some operations but will inherently increase the cost of sampling versus only one sample location. There is also an opportunity to evaluate the spatial consistency and variance of the 3P transects when using images from different phenological stages, prior seasons, or different aerial providers or resolutions and will be the topic of a future paper.

## Conclusion

While some of the values extracted from the three pixel transects fell away from the peak of the respective histograms, most were still within  $\pm 1^\circ$  brix of the field averages and all were within the standard deviation of each of the field averages. This method could be useful to growers, vineyard managers, or wineries interested in a repeatable, robust, cost-effective sampling strategy for understanding how vineyard variability could affect the winemaking process.

## Acknowledgements

This work was funded by E&J Gallo Winery, The University of Adelaide, and CSIRO. The authors would like to thank the Winegrowing Research staff at E&J Gallo Winery for their help and support in the collection, processing, and analysis of the collected grape samples.

## Literature Cited

1. Baluja, J., Diago, M.P., Goovaerts., and Tardaguila, J. (2012) Assessment of the spatial variability of anthocyanins in grapes using a fluorescence sensor: relationships with vine vigour and yield. *Precision Agriculture* 13, 457-472.
2. Bramley, R.G.V. (2005) Understanding variability in winegrape production systems 2. Within vineyard variation in quality over several vintages. *Australian Journal of Grape and Wine Research* 11, 33–42.
3. Bramley, R.G.V., Ouzman, J. and Boss, P.K. (2011a) Variation in vine vigour, grape yield, and vineyard soils and topography as indicators of variation in the chemical composition of grapes, wine and wine sensory attributes. *Australian Journal of Grape and Wine Research* 17, 217–229.
4. Bramley, R.G.V., Ouzman, J., and Thornton, C. (2011b) Selective harvesting is a feasible and profitable strategy even when grape and wine production is geared towards large fermentation volumes. *Australian Journal of Grape and Wine Research* 17, 298–305.

5. Dorin, B., Reynolds, A.G., Jollineau, M., Lee, H., and Shemrock, A. (2022) Utilization of unmanned aerial vehicles for zonal winemaking in cool-climate Riesling vineyards. *OENO One* 56, 327-341.
6. Fiorillo, E., Crisci, A., De Filippis, T., Di Gennaro, S.F., Di Blasi, S., Matese, A., Primicerio, J., Vaccari, F.P. and Genesio, L. (2012) Airborne high-resolution images for grape classification: changes in correlation between technological and late maturity in a Sangiovese vineyard in Central Italy. *Australian Journal of Grape and Wine Research* 18, 80–90.
7. Gorelick, N., Hancher, M., Dixon, M., Ilyushchenko, S., Thau, D., and Moore, R. (2017) Google Earth Engine: Planetary-scale geospatial analysis for everyone. *Remote Sensing of Environment* 202, 18-27.
8. Gutiérrez, S., Tardaguila, J., Fernandez-Novales, J. and Diago, M.P. (2019) On-the-go hyperspectral imaging for the in-field estimation of grape berry soluble solids and anthocyanin concentration. *Australian Journal of Grape and Wine Research* 25, 127–133.
9. Hall, A., Lamb, D.W., Holzapfel, B., and Louis, J. (2002) Optical remote sensing applications in viticulture – a review. *Australian Journal of Grape and Wine Research* 8, 36-47.
10. Hall, A., Lamb, D.W., Holzapfel, B.P. and Louis, J.P. (2011) Within-season temporal variation in correlations between vineyard canopy and winegrape composition and yield. *Precision Agriculture* 12, 103–117.
11. Meyers, J.M., Dokoozlian, N., Ryan, C., Bioni, C. and Vanden Heuvel, J.E. (2020) A new, satellite NDVI-based sampling protocol for grape maturation monitoring. *Remote Sensing* 12, 1159.
12. Minasny, B., McBratney, A.B. and Whelan, B.M. (2005) VESPER version 1.62 (Australian Centre for Precision Agriculture, University of Sydney: Sydney, NSW, Australia). [www.sydney.edu.au/agriculture/pal/software/vesper.shtml](http://www.sydney.edu.au/agriculture/pal/software/vesper.shtml)
13. R Core Team (2023) R: a language and environment for statistical computing (R Core Team: Vienna, Austria) <https://www.R-project.org/>
14. Sams, B., Bramley, R.G.V., Sanchez, L., Dokoozlian, N., Ford, C., and Pagay, V. (2022a) Characterising spatio-temporal variation in fruit composition for improved winegrowing management in California Cabernet Sauvignon. *Australian Journal of Grape and Wine Research* 28, 407-423.
15. Sams, B., Bramley, R.G.V., Sanchez, L., Dokoozlian, N., Ford, C., and Pagay, V. (2022b) Remote sensing, yield, physical characteristics, and fruit composition variability in Cabernet Sauvignon vineyards. *American Journal of Enology and Viticulture* 73, 93-105 .
16. Sozzi, M., Kayad, K., Marinello, F., Taylor, J. and Tisseyre, B. (2020) Comparing vineyard imagery acquired from Sentinel-2 and unmanned aerial vehicle (UAV) platform. *OENO One* 54, 189–197.

17. Taylor, J.A., Sanchez L., Sams, B., Haggerty, L., Jakubowski, R., Djafour, S., and Bates, T. (2016) Evaluation of a commercial grape yield monitor for use mid-season and at-harvest. *Journal internationale des sciences de la vigne et du vin* 50(2)
18. Trought, M.C.T. and Bramley, R.G.V. (2011) Vineyard variability in Marlborough, New Zealand: characterising spatial and temporal changes in fruit composition and juice quality in the vineyard. *Australian Journal of Grape and Wine Research* 17, 79–80.